

Chapter 2

Synthesis and Characterization of a Silica Membrane Supported on Porous Vycor

2.1. Introduction

In this chapter, the synthesis, characterization, and gas permeation properties of a silica membrane supported on porous Vycor are presented. The silica membrane, referred to as Nanosil, was prepared by forming a thin silica layer on porous Vycor using the chemical vapor deposition (CVD) technique. The silica precursor used was tetraethylorthosilicate (TEOS), and the membrane layer deposition was carried out by decomposing TEOS at 873 K in inert atmospheric pressure. The schematic of the silica deposition process was shown in Fig. 2.1.

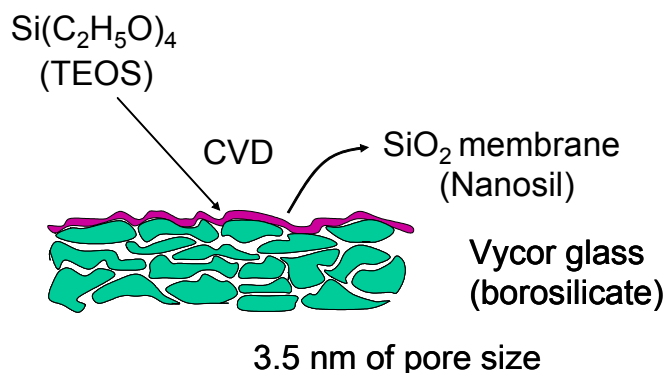


Figure 2.1. Illustration of the silica membrane preparation method

The Nanosil membrane displayed high selectivity to hydrogen while maintaining the permeability of the original Vycor material. The permeability properties of the Nanosil and Vycor glass membranes were compared, and atomic force microscopy (AFM) images of both membrane surfaces were obtained at nanometer resolution. These images were the first application of AFM to this system, and allowed visualization of the plate-like structure of the surface. The AFM measurements were obtained in the laboratory of Professor Y. Iwasawa at The University of Tokyo by S. Sugiyama and K. Fukui.

2. 2. Experimental

The Vycor glass membrane was purchased commercially (Corning 7930) and had a nominal pore size of 4 nm. It had a tubular geometry with an OD of 10 mm and a thickness of 1 mm. The Nanosil membrane was prepared by a chemical vapor deposition (CVD) modification of the Vycor membrane which resulted in the formation of a thin layer of silica on the surface of the Vycor glass. Briefly, the CVD procedure was carried out in a concentric tubular apparatus with the outer tube consisting of solid quartz and the inner tube holding the Vycor glass. The Vycor glass itself was a 4 cm long central section attached to two pieces of quartz tubing by glass blowing joints. The schematic of the CVD reactor system is shown in Fig. 2.2. Flows of argon were established on the outer shell side ($20 \mu\text{mol/s}$) and inner tube side ($8 \mu\text{mol/s}$) and the temperature was raised to 873 K. (Flow rates in $\mu\text{mol/s}$ can be converted to cm^3 (NTP)/min by multiplication by 1.5). A flow of tetraethyl orthosilicate (TEOS, Aldrich, 98%) introduced through a bubbler (at 298 K) using Ar ($3 \mu\text{mol/s}$) as the carrier gas, was added to the tube side Ar flow and passed over the Vycor membrane for 12 h.

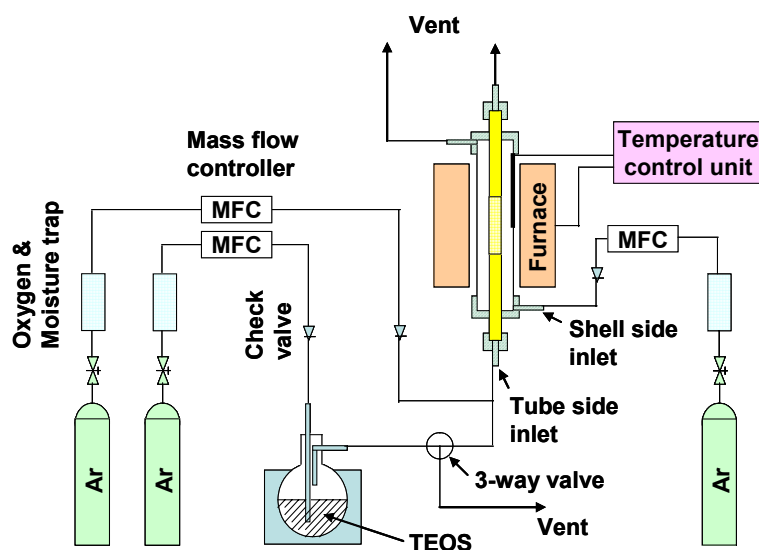


Figure 2.2. Schematic of the CVD reactor system.

Individual gas permeabilities were determined by flowing $20 \mu\text{mol s}^{-1}$ of the pure gas at 123 kPa in the shell side and measuring the tube side (at atmospheric pressure) flow rate using a sensitive bubble flow meter. The permeance (P_i) ($\text{mol m}^{-2} \text{s}^{-1} \text{Pa}$) of the individual gases (i) were

obtained from the expression $P_i = Q_i/A\Delta P$, where Q_i is the flow rate on the tube side (mol s^{-1}), A is the cross sectional area (m^2) of the membrane available for diffusion, and ΔP is the pressure difference (Pa) between the shell and tube side. Characterization of the membranes by N_2 physisorption was carried out in a volumetric unit (Micromeritics ASAP 2000). Pore size distributions were obtained by applying the Barrett, Joyner and Halenda (BJH) method to the nitrogen desorption isotherm.

AFM measurements were performed with a high vacuum scanning probe microscope (JEOL JSTM 4200X). The samples were evacuated inside the microscope for two days prior to measurements to remove water layers on the surface of the samples. Without this evacuation, the water layers degraded the quality of the sample images. A cantilever with a pyramidal tip of SiN (Olympus) was used as the probe sensor. The force constant of the lever was 0.02 N m^{-1} . The surface structure of the sample was determined in the contact mode to obtain the topography. For this measurement a constant force of $\sim 0.3 \text{ nN}$ was set between the tip and the sample.

2.3. Results and Discussion

The pore size distribution of the Vycor membrane determined by porosimetry was unimodal and narrow, with a mean pore size of 3.6 nm and a standard deviation of 0.5 nm (Fig. 2.3). There was no change in this distribution after deposition of the silica layer to form the Nanosil membrane. Evidently the pore volume contributed by the silica was negligible or inaccessible to the nitrogen adsorbent.

The pore size of 3.6 nm fell in the region of Knudsen diffusion (equation 2.1) [i],

$$F_K \frac{\varepsilon d_p}{\tau L} \left(\frac{8}{9\pi MRT} \right)^{1/2} = C \left(\frac{1}{T} \right)^{1/2} \quad (2.1)$$

$$C = \frac{\varepsilon d_p}{\tau L} \left(\frac{8}{9\pi MR} \right)^{1/2} \quad (2.2)$$

In these equations F_K is the permeance ($\text{mol m}^{-2}\text{s}^{-1}\text{Pa}^{-1}$), ε is the porosity, d_p is the pore diameter (m), τ is the tortuosity, L is the membrane thickness (m), R is the gas constant ($8.314 \text{ J mol}^{-1}\text{K}^{-1}$), T is the temperature (K), and M is the molecular weight (kg mol^{-1}).

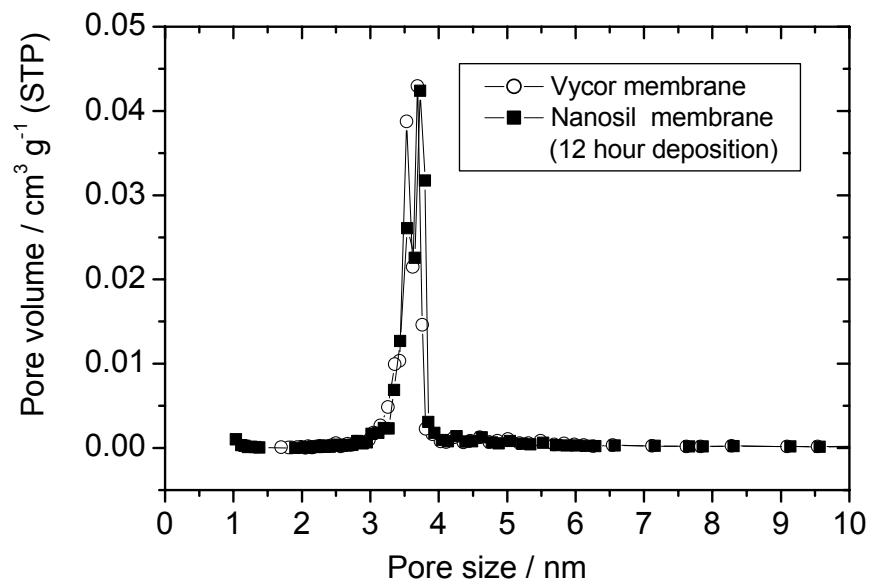


Figure 2.3. Pore size distributions of the Vycor and Nanosil membranes.

For the Vycor membrane it was found that the permeability of the series of gases comprising CO₂, CO, Ne, CH₄, He, and H₂ followed roughly the Knudsen equation. The effect of mass showed the expected inverse square root of molecular mass ($M^{-1/2}$) dependence (Fig. 2.4). The effect of temperature was close to that expected from the Knudsen equation which predicts an exponent of -0.50 . The individual gases (Fig. 2.5, open points) gave fits with exponents of -0.458 for He, -0.463 for H₂, and -0.458 for Ne.

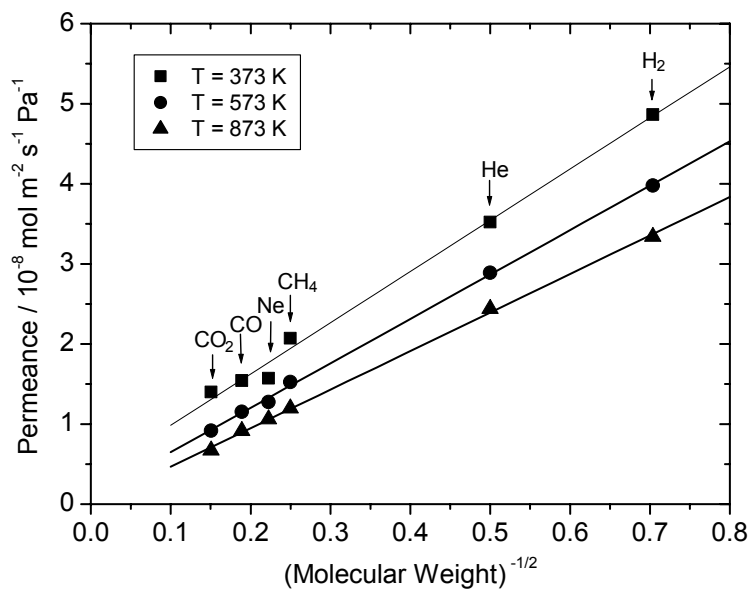


Figure 2.4. Permeance of light gases through the Vycor membrane.

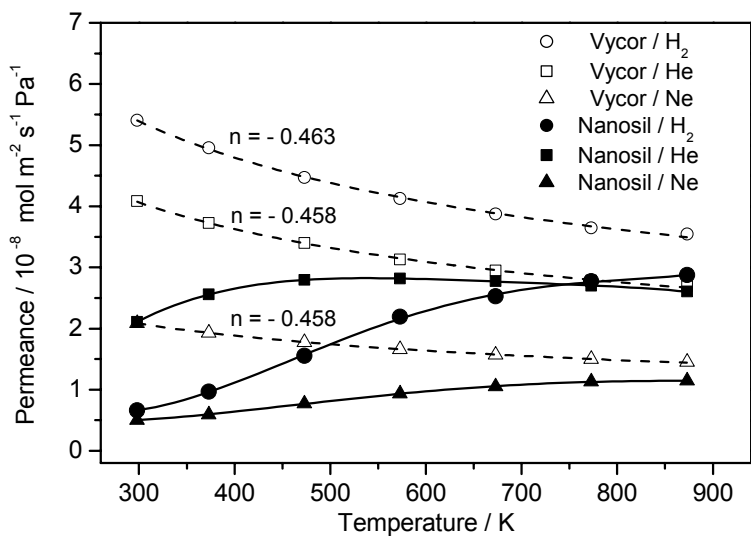


Figure 2.5. Temperature dependence of permeability through the Vycor and Nanosil membranes.

These slight deviations from the expected value of -0.50 indicated that the transport process involved some interactions of the gases with the pore walls. The curves connecting the open points (Fig. 2.5) are the actual theoretical curves. The parameters are given in Table 2.1, including the χ^2 values, which confirm the excellence of fit.

Values of the group $C = \frac{\varepsilon d_p}{\tau L} \left(\frac{8}{9\pi MR} \right)^{1/2}$ (Equation 2) were calculated using as parameters, $\varepsilon = 0.28$ [ii,iii], $d_p = 3.6 \times 10^{-9}$ m, $\tau = 5.9$ [iv,v], $L = 1.1 \times 10^{-3}$ m. All of these are experimental quantities and the excellent agreement between calculated and measured C values without adjustable parameters indicate that the Knudsen model is a reasonable description of the permeance of the gases through the Vycor membrane.

Table 2.1. Parameters in the Knudsen equation

Gas	n	C (exptl) mol K ^{1/2} /m ² sPa	C (calc) mol K ^{1/2} /m ² sPa	χ^2
He	-0.458	5.353×10^{-7}	4.529×10^{-7}	2.556×10^{-19}
H ₂	-0.463	7.554×10^{-7}	6.392×10^{-7}	4.820×10^{-19}
Ne	-0.458	2.384×10^{-7}	2.018×10^{-7}	2.971×10^{-19}

The permeance behavior of the Nanosil membrane displayed a completely different mass and temperature dependence from that of the Vycor membrane. Regarding mass, there was no inverse square root dependence. In fact, no other molecules aside from He, H₂ and Ne were observed to pass across the Nanosil membrane. The permeability order of these gases was He > H₂ > Ne which did not depend on the kinetic diameter (0.26 nm for He, 0.275 for Ne, and 0.289 nm for H₂ [vi]) or mass of the molecules.

Regarding temperature, the Nanosil membrane displayed a completely different behavior from the Vycor substrate (Fig. 2.5, solid points). Instead of decreasing as temperature is

increased, the permeability of the Nanosil membrane increased. This is consistent with an activated diffusion mechanism. However, the increase was not unlimited, the permeability curves of the three gases increased at first but then bent over as they neared the Vycor limit. This is because the transport of species occurs in series through the Vycor and Nanosil portions, and eventually, at high temperatures the transport is limited by the Vycor. The curve for He even showed a decline, in line with the behavior for the Knudsen mechanism. The permeability of H₂ showed a dramatic increase above 400 K, eventually resulting in a greater permeability than even He. This is remarkable given that the kinetic diameter of H₂ is larger than that of He.

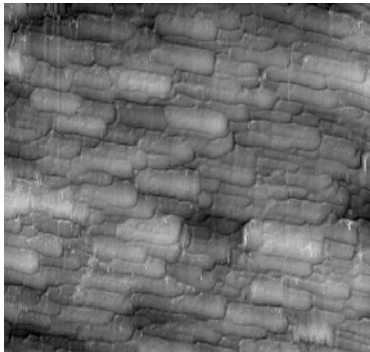
In order to obtain better insight into the nature of the Nanosil membrane, its structure was probed with atomic force microscopy. A direct comparison was made with the Vycor glass membrane. Since its introduction [vii] AFM has been increasingly used to study inorganic materials [viii] at unprecedented resolution. The technique offers considerable advantages over electron microscopy in its two common forms to study membranes. In the case of scanning electron microscopy (SEM) the resolution is not high enough, and in the case of transmission electron microscopy (TEM) sample preparation, e.g., by replica techniques, is difficult and can introduce artifacts [ix]. For membranes AFM has been applied mostly for the study of polymeric membranes [x,xi,xii], although there have been reports of its use for the investigation of inorganic micro- and ultra-filtration membranes [ix, xiii].

Results for the Vycor and Nanosil membranes obtained in the present study are shown in Fig. 2.6. The top panels show images of the Vycor glass at increasing magnification. At low magnification (500 x 500 nm²) the surface structure of the Vycor membrane was found to consist of rectangular, plate- or tile-like elements. These elements overlapped each other like shingles on a roof, but in a random manner. At first glance most of the plates appeared to be of a large size, but closer examination revealed that there were also regions between these plates containing smaller elements. Thus, the distribution of sizes appears to be bimodal. A rough count of approximately 20 plates revealed that the dimensions of the larger plates are 90 ± 15 nm x 30 ± 7 nm, while those of the smaller tiles are 30 ± 10 nm x 16 ± 4 nm. At higher magnification (100 x 100 nm²) the edges between plates are visible, constituting what appear to be the pore entrances. From the highest magnification (50 x 50 nm²) image the dimensions of the edge features were

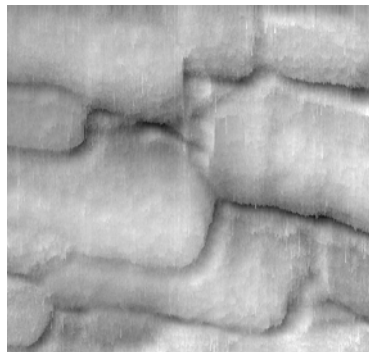
about 4 nm, about the order of the average pore size (3.6 nm) obtained from porosimetry. Porosimetry also indicated that the pores were slit- or rectangular-shaped supporting the view that the pores were formed by the spaces between the plates.

The bottom panels (Fig. 2.6) show images of the Nanosil membrane. At low magnification ($500 \times 500 \text{ nm}^2$) the surface structure is now seen to consist of globular, elongated particles which again overlap each other. Compared to the plate-like elements in the Vycor, these particles were more rounded and are larger, with dimensions of $110 \pm 20 \text{ nm} \times 50 \pm 13 \text{ nm}$. At high magnification ($100 \times 100 \text{ nm}^2$) it can be seen that the fine features between particles have been largely eliminated. The results are consistent with the deposition of a fine silica layer on top of the Vycor membrane. This is shown in the lower right of Fig. 2.6. The thickness of the layer was approximated as 10 nm, one-half the difference between the dimensions of the Vycor plates and the Nanosil globules. This thickness was consistent with the permeability properties of the Nanosil, and was much smaller than the thickness (500 nm, 0.5 μm) achieved by conventional CVD of SiO_2 [xiv]. The results presented here for the characterization of the Vycor and Nanosil membranes advance our present understanding of the materials by providing high resolution images of the surface structure not achievable by such techniques as small angle diffraction and electron microscopy [xiv,xv].

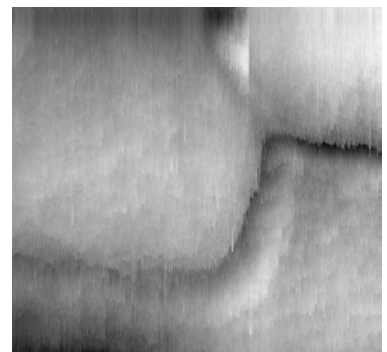
Untreated Vycor



500 x 500 nm²

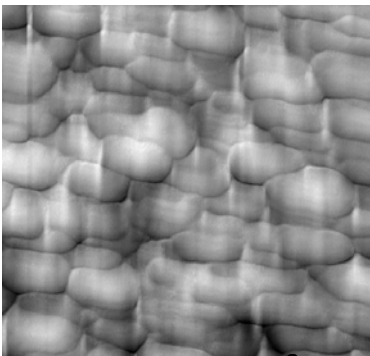


100 x 100 nm²

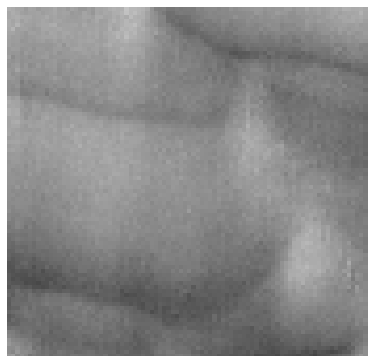


50 x 50 nm²

Nanosil



500 x 500 nm²



100 x 100 nm²

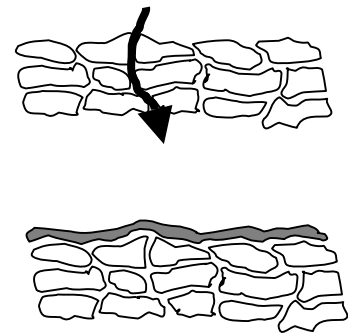


Figure 2.6. Atomic force micrographs of the Vycor and Nanosil membranes.

2.4. Conclusions

A new type of composite silica membrane denoted as Nanosil was prepared by the chemical vapor deposition of a silica precursor on Vycor glass. The permeation properties of this membrane towards the small gas molecules H₂, He, Ne, CH₄, CO, and CO₂ were investigated. It was found that the permeation mechanism changed from a Knudsen type mechanism for the Vycor glass to an activated diffusion mechanism for the Nanosil membrane. Only H₂, He, and Ne permeated through the Nanosil membrane. Atomic force microscopy

indicated that the Vycor consisted of plate like structures of tens of nanometers in size, and that the Nanosil membrane was formed as a thin silica layer of about 10 nm thickness on top of this structure.

References

- [i]. M. Knudsen, *Ann. Phys.* **1909**, 28, 75.
- [ii]. C. E. Megiris, J. H. E. Glezer, *Ind. Eng. Chem. Res.* **1992**, 31, 1293.
- [iii]. R. A. Levy, E. S. Ramos, L. N. Krasnoperov, A. Datta, K. M. Grow
J. Mater. Res. **1996**, 11, 3164.
- [iv]. C. N. Satterfield, T. K. Sherwood, *The Role of Diffusion in Catalysis*,
Addison-Wesley, Reading, Massachusetts, **1963**.
- [v]. A. B. Shelekin, A. G. Dixon, Y. H. Ma, *J. Membr. Sci.* **1993**, 83, 181.
- [vi]. D. W. BRECK, *Zeolite Molecular Sieves*, John Wiley, New York, **1974**.
- [vii]. G. Binnig, C. F. Quate, C. H. Gerber, *Phys. Rev. Lett.* **1986**, 12, 930.
- [viii]. M. A. Ray, G. E. McGuire, I. H. Musselmann, R. J. Nemanich, D. R. Chopra,
Anal. Chem. **1991**, 63, 99R.
- [ix]. A. Bottino, G. Capannelli, A. Grosso, O. Monticelli, O. Cavalleri, R. Rolandi,
R. Soria, *J. Membr. Sci.* **1994**, 95, 289.
- [x]. A. Chahboun, R. Coratger, F. Ajustron, J. Beauvillain, *Ultramicroscopy*
1992, 41, 235.
- [xi]. T. Miwa, M. Yamaki, H. Yoshimina, S. Ebina, K. Nagayama, *Jpn. J. Appl.*
Phys. **1992**, 31, L1495.
- [xii]. P. Dietz, P. K. Hansma, O. Inacker, H. D. Lehman, K. H. Herrmann,
J. Membr. Sci. **1992**, 65, 101.
- [xiii]. W. R. Bowen, N. Hilal, R. W. Lovitt, P. M. Williams, *J. Membr. Sci.* **1996**, 110, 233.
- [xiv]. M. Tsapatsis, G. Gavalas, *J. Membr. Sci.* **1994**, 87, 281.
- [xv]. P. Levitz, G. Ehret, S. K. Sinka, J. M. Drake, *J. Chem. Phys.* **1991**, 95, 6151.